



## CHANGE DETECTION FOR MAP UPDATING USING VERY HIGH-RESOLUTION SATELLITE IMAGES

Yasser G. Mostafa<sup>1</sup>, Nasser A. Mohamed<sup>2</sup>, Farrag A. Farrag<sup>3</sup>

<sup>1</sup>Civil Eng. Dpt. Faculty of Engineering, Sohag University. [yasser\\_g\\_m@yahoo.com](mailto:yasser_g_m@yahoo.com)

<sup>2</sup>Civil Eng. Dpt. Faculty of Engineering, Sohag University. [naserahmed@eng.sohag.edu.eg](mailto:naserahmed@eng.sohag.edu.eg)

<sup>3</sup>Civil Eng. Dpt. Faculty of Engineering, Assiut University. [farrag@aun.edu.eg](mailto:farrag@aun.edu.eg)

Received 5 April 2021; Revised 17 April 2021; Accepted 23 May 2021

### Abstract

The earth surface changes continuously due to natural causes and human activities. New generations of satellite sensors, such as WorldView and GeoEye, provide new data to better delineate, track, and visualize changes in land cover. Several classes are used in the satellite images. All artifacts with elevations greater than the ground surface (buildings in particular) may appear in the wrong location. The correction of buildings position is an important task for mapping applications. The main aim of this study is to introduce a change detection approach using very high-resolution satellite images (VHR) for map updating. In this approach, an approximated method for building relief displacement correction was developed.

In this paper, image preprocessing was carried out and the information content of the satellite image was evaluated. Then change detection between GeoEye-1 image and Sohag map was carried out using post-classification comparison technique. After that, the change map result was divided into two classes: building and non-building. All objects were transformed from raster to vector format. For building objects, the height was estimated. A python

code was written to calculate relief displacement using buildings' height and shadow length. The vector layer was added to update the reference map. The results showed the ability of very high-resolution satellite images for updating large-scale maps in Egypt. Also, the approximated method for building relief displacement correction is a promising method. It has RMSE accuracy of 0.95m.

**Keywords:** map updating, change detection, relief displacement.

## 1. Introduction

Land cover change is considered one of the essential components of the current techniques for natural resource management and monitoring of environmental changes [1]. Global and environmental change studies have widely recognized the value of characterizing, quantifying, and tracking land cover changes [2]. Automatic extraction of buildings from remote sensing images plays a critical role in urban planning and digital city construction applications [3]. With the fast development of satellite image technology, a significant number of very high-resolution (VHR) observational remotely sensed satellites, such as WorldView and QuickBird, have been launched in recent decades, introducing new challenges and possibilities for data processing by remote sensing [4]. Satellite image features are classified into two categories; the first features are correctly placed on the map (non-building features). The second was objects with elevations greater than the surface of the ground (in particular, buildings) that appear due to their relief displacement in a wrong location. For mapping applications, the correction of the location of buildings is therefore, an essential activity. The image can be correctly geocoded by using this method of geometrical correction [5].

Comber Alexis et. al, (2012) [6] Provides a rule-based method to determine the height of the building by shadow, classifying the shadow of the building based on the relative density within scene characteristics, spatial context, rules which that geo-located images of the study area are empirically calculated. For the study, which may involve an approximate measure of building height, this method was suitable. Automatic feature detection using object-based classification and shadow information in multispectral images of a very high resolution was presented by Benarchid

et al, (2013) [7]. Zhang (2019) [8] uses Local Binary Pattern (LBP) object-oriented feature maps to detect changes in VHR images.

In this research for map updating, a change detection technique between map and very high-resolution satellite image was introduced. Also, an approximated method for relief displacement correction was developed to correct the building's rooftops position for accurate map updating. The rest of this paper is organized in the following sections. Methodology, study area, data used, and image preprocessing steps are introduced in section 2. Next, the information content of the GeoEye-1 image was evaluated in section 3. The change detection between image and map will be illustrated in section 4. Section 5 depicts an approximated method for relief displacement correction for buildings. Map updating is described in section 6. Discussion is introduced in section 7. Finally, the conclusion is discussed in section 8.

## **2. Methodology**

For several areas of research, the updating of land cover maps from satellite data in a timely manner is essential. In this study image to map change detection is carried out in six steps (figure 1). First, image preprocessing was done through geometric correction, data fusion, and shadow restoration. Then information content of the satellite image was evaluated. After that, the post-classification comparison change detection method was used to detect the changed features. The change map was transformed from raster to vector and divided into two sections: building and non-building. For building objects, the height was estimated and an approximated method for relief displacement correction was developed. A python code was written to move rooftops to their correct position. Finally, the new data was added for updating the reference map.

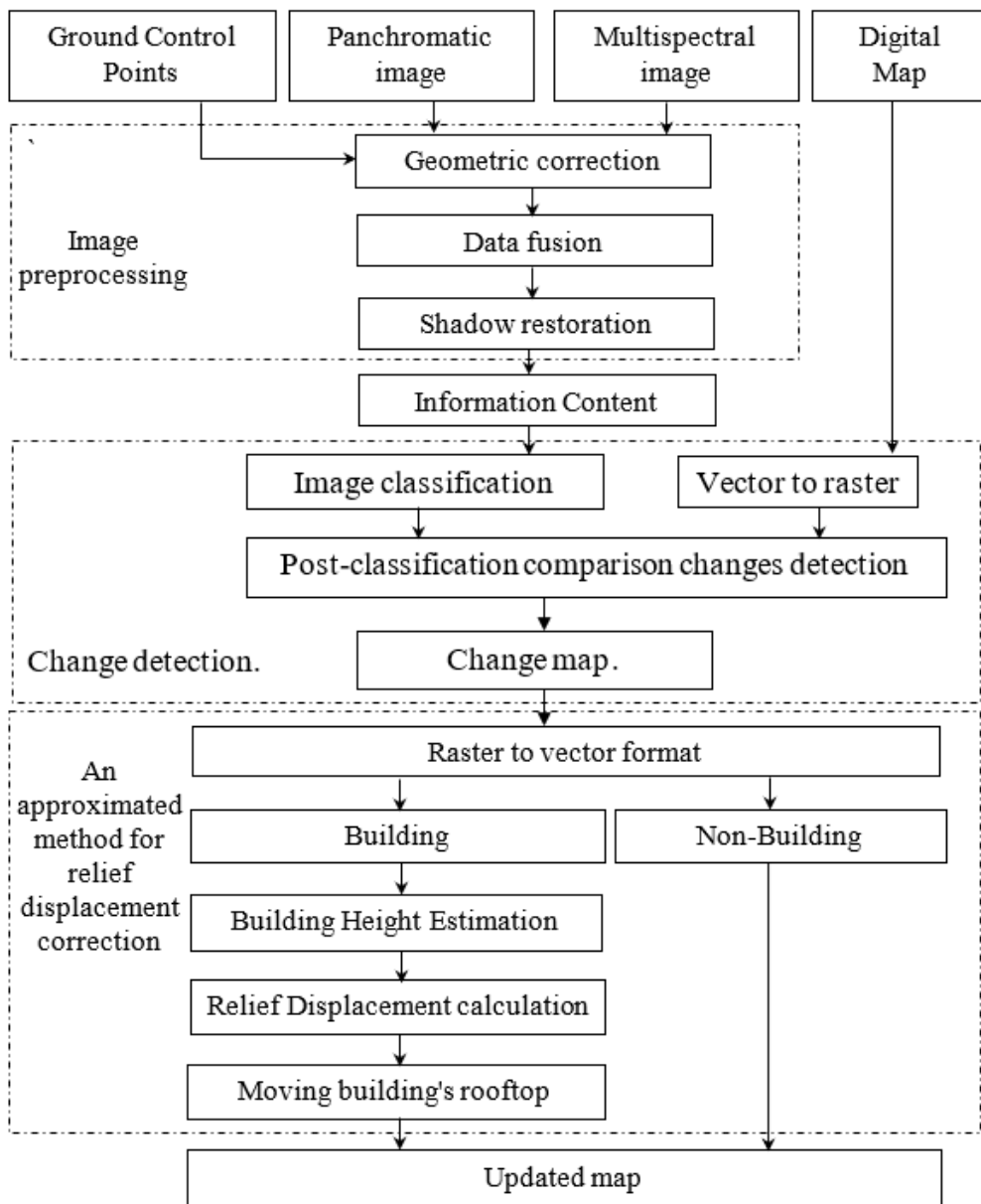
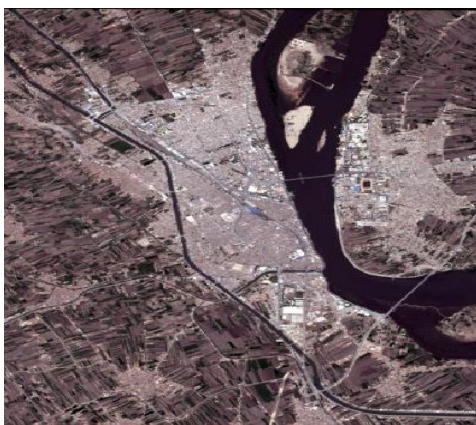


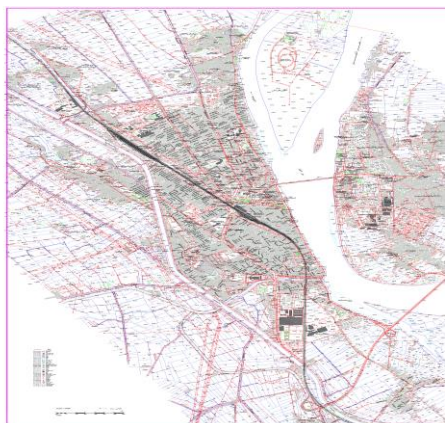
Figure 1: methodology flow chart.

## 2.1. Study area and Data used.

The study area lies in Sohag City, the capital of Sohag governorate which is one of the ancient capitals of Egypt. It lies between  $26^{\circ}6'7.25''\text{N}$ , to  $27^{\circ}21'50.03''\text{N}$  and  $31^{\circ}18'2.6''\text{E}$ , to  $32^{\circ}46'57.71''\text{E}$ . Sohag governorate extends for 125 Km along the Nile River. For this research GeoEye-1 Panchromatic (0.46m) and Multispectral (1.84m) images acquired on 24th May 2014 at an angle of 19.16 degrees are used (figure 2). Also, a large-scale 1:5000 topographic map for the study area is used. Figure 2 shows a window from the map corresponding to the study area. The topographic maps were compiled from aerial photographs in 2006 and produced by the Egyptian General Authority of Survey.



(a) GeoEye-1 image



(b) Topographic map at scale 1: 5000

Figure 2. Sohag city and the surrounding

## 2.2. Data preprocessing

To present the satellite images in a more appropriate form for better interpretation and extracting the maximum information, three stages were performed: image geo-referencing, image fusion, and shadow restoration.

### 2.2.1. Geometric Correction

To preprocess remotely sensed data and eliminate geometric distortion, geometric correction is required. The GeoEye-1 image was delivered georeferenced according to the Universal Transverse Mercator (UTM)

projection, Northern Hemisphere, zone 36, and World Geodetic System (WGS84) Datum. Registration was done by geo-referencing the images to the Egyptian Transverse Mercator (ETM) map projection. Using SOKKIA GRX-2 with precision (10 mm + 1 ppm), twenty-five Ground Control Points (GCPs) are calculated to be used for image geometric correction. In a nearly uniform distribution, GCPs were taken. The third-order polynomial method provides high accuracy with RMS errors at 0.541 m checkpoints. This result meets technical specifications of the Egyptian Survey Authority (the horizontal error does not exceed 1.5 meters as a maximum mean square error not more than 10% of the number of points tested, compared to the actual coordinates of these points) [9]

### 2.2.2. Image fusion:

The fused images offer improved interpretation capabilities and performance that is more accurate. There are several techniques for image fusion, such as Intensity-Hue-Saturation (IHS), Brovey Transform, wavelet transform, High-Pass Filter (HPF) technique, and Hyperspherical Color Space (HCS). HPF method provides better results than others so it was used in this research [10].

### 2.2.3. Shadow restoration

Shadow is considered as a key barrier to satellite imagery, limiting the precision of identification of changes and extraction of features [11]. The restoration of shadows is an important step in eliminating or reducing the shadow effect. The process of Shadow restoration consists of two main steps: identification and compensation. The Shadow Detector Index (SDI) proposed by Mostafa and Abdelhafiz [12] was used in this research. The SDI index is determined using the following formula for each image pixel:

$$SDI = \left( \frac{(I - PC_1) + 1}{((G - B) * R) + 1} \right) \dots\dots\dots (1)$$

where  $PC_1$ ,  $R$ ,  $G$ , and  $B$  are normalized components of the first principal component, red band, green band, and blue band, respectively.

In the index histogram, large values of the shaded regions are obtained. To detect the shadow field, image thresholding is carried out. Using the surrounding shadow data, shadow areas can be improved [13]. In this work, for shadow restoration, the Linear Correlation Correction (LCC) method is chosen. In the LCC approach, shadow brightness can be restored by a linear relationship as follows:

$$DNn = \left( \frac{\sigma_{non-shadow}}{\sigma_{shadow}} \right) (DN_{shadow} - \mu_{shadow}) + \mu_{non-shadow} \dots (2)$$

where  $DNn$  is the digital number of the corrected image.  $\sigma_{shadow}$  and  $\sigma_{non-shadow}$  are the standard deviation of the shadow and non-shadow image, respectively.  $\mu_{shadow}$  and  $\mu_{non-shadow}$  are the mean of shadow and non-shadow image, respectively.  $DN_{shadow}$  is the digital number of the shadow image. This step was applied for the GeoEye-1 image using model maker in ERDAS IMAGEN 2013 as shown in figure 3.

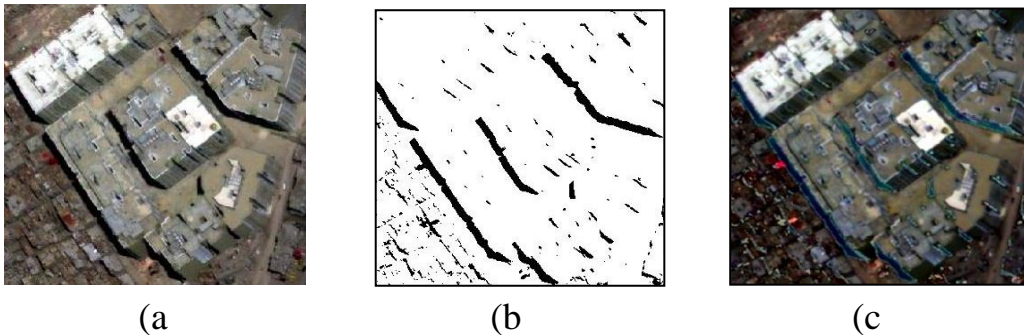


Figure 3: shadow restoration a) original image b) shadow detection and c) shadow compensation

### 3. Information Content of GeoEye-1 Image

Information content means the ability to extract different object layers from space images like roads, vegetation, and buildings [14]. For clear detection, the ground object has to be identified with two to four pixels on a map and a minimum of approximately 0.05 to 0.1 mm GSD ( $[0.25/4]$  to  $[0.25/2]$ ) is needed according to the Egyptian Survey Authority, topographic maps [9]. A topographic map, with a scale of

1:5000, can be created with 0.46 m GSD provided by GeoEye-1 fused image ( $0.46 \text{ m} / 0.1 \text{ mm} = 4600 > 5000$ ) [15]. In this study, a reference 1:5000 scale map is used to study the information content of the GeoEye-1 image and determine its suitability through visual inspection for updating large-scale maps. The features which exist in the study area and are represented in the 1:5000 map is considered and evaluated. The required information content for 1:5000 scale maps may be divided into four main categories, cultural feature, transportation, Vegetation, and hydrological. In table 1 objects in the GeoEye-1 image are classified based on their level of detection and recognition. In this case, if the object can be detected, recognized sharply and easily, then it is recognized as "Perfect". If the level was lower than, it is identified as "Good". If an object is only identified or detected, then it is put into the class of "Medium". If the level was very low, then it is "Poor". If the object is not available in the image, it is categorized as "Not available" [16].

#### **4. Post-classification comparison change detection technique.**

A logical comparison is made between two independent classified images by Post-Classification Comparison (PCC) technique. To detect the changes that occurred between the GeoEye-1 image and the Sohag map, an object-based classification technique was used to classify the GeoEye-1 image. The satellite image was segmented using the Multiresolution segmentation method with scale parameter 50. Then training areas were selected. After that, the nearest neighbor classification was applied as shown in figure 4 using recognition software.

Object-based classification of GeoEye-1 image has high overall accuracy equal to 90.67% and Overall Kappa equal to 0.88. For the individual classes, the producer's accuracy is ranging from 82.43% to 100.00%. And the user's accuracy is ranging from 83.64% to 96.83%. The producer's accuracy for vegetation has less percentage 82.43%. Sohag map was transformed from vector to raster and each feature was given a specific color as shown in figure 4.

Table 1: Evaluation of GeoEye-1 information content for 1:5000 maps.

Information content of 1:5000 map			Information content of pansharpened GeoEye 1 image										
			Detection					Identification					
			Perfect	Good	Medium	Poor	N.A.	Perfect	Good	Medium	Poor	N. A.	
Cultural Feature	Buildings	Isolated building	X					X					
		Under construction	X						X				
		Boundaries of high density and rural area	X					X					
		Government building	X							X			
		Mosque/Church/Jewish	X					X					
		School	X						X				
		Hospital	X							X			
	Recreational	Police station/	X							X			
		Park/Garden	X					X					
		Playground	X					X					
		Swimming Pool	X					X					
		Stadium	X					X					
	Other	Cemetery Muslim/Christian	X						X				
Electric power line				X					X				
Wall/Fence			X					X					
Transport	Road class	Main Paved Road	X					X					
		Secondary Paved Road	X					X					
		Unpaved Road		X					X				
		track		X					X				
	Railway track	Railway double track	X					X					
		Railway single track	X					X					
	Transport Terminal	Railway Station	X					X					
	Others	Bridge	X					X					
Tunnel			X					X					
Vegetation	Agriculture	Cultivated area		X					X				
		Single		X					X				
	Tree/ Palm	Grove	X						X				
		Hedge	X						X				
Hydrology	Water body	River	X					X					
		Water Tank	X					X					
		Drain	X					X					

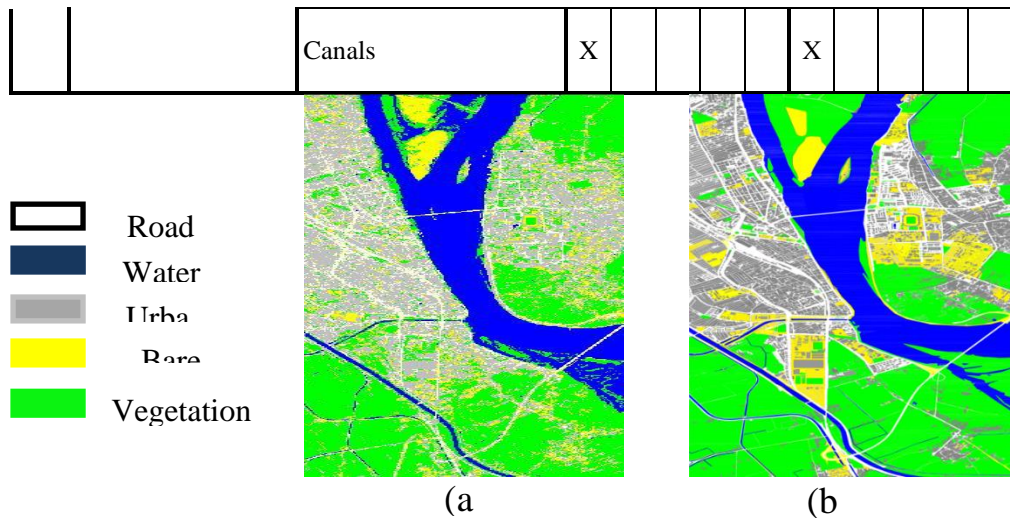


Figure 4: Classification images a) GeoEye-1 image b) Sohag map

The change map resulted as shown in figure 5 was classified into eight classes: No Change (NC), Vegetation to Urban (V-U), Vegetation to Road (V-R), Vegetation to Bare soil (V-B), Vegetation to Water (V-W), Bare soil to Urban (B-U), Bare soil to Vegetation (B-V) and Water to Vegetation (W-V).

Accuracy assessment applied (overall accuracy and kappa coefficient) to evaluate the accuracy of PCC method result. To determine the accuracy of the change detection process, the number of samples of the reference data is determined based on a rule of thumb that recommends that at least 50 samples per class are included in the error's matrix. The number of samples for each category might be adjusted based on the relative importance of that category for a particular application [17]. The study area contains eight change classes, so  $50 \times 8 = 400$  samples can be considered. To satisfy the importance and variability within each category 100 samples were added over 400 samples to be 500 samples (distributed as 118 for NC, 51 for V-U, 54 for V-R, 62 for V-B, 53 for V-W, 54 for B-U, 54 for B-V and 54 for W-V).

Post classification comparison technique shows misclassification in some of the classes such as V – R which is located at the medal of image. PCC technique has Overall Accuracy of 89.60% and Overall Kappa 0.88

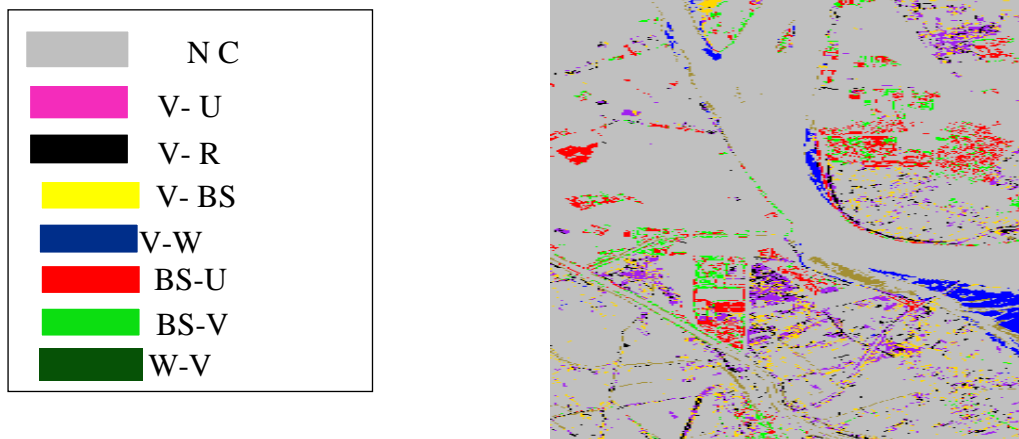


Figure 5: The change map of post-classification comparison technique.

The quantitative analysis was carried out on the resulting change map. The area of each class was computed and given in Table 2. Most of the changes were bare soil to urban, vegetation to water, and vegetation to urban, located in the west and south of the study area. The transformation from bare soil to urban and vegetation to urban was occurred due to urban expansion and population increase. The transformation from vegetation to water was occurred due to the increase of water level at the Nile River at that time, so the island was covered by water. The highest percentage of change was found in class bare soil to urban (2.92 %). The expansion of cities and villages in Egypt must be monitored almost annually to control the illegal construction of buildings.

The accurate location of buildings in very high-resolution (VHR) images has attracted considerable attention in remote sensing because the information is highly related to human activities in urban planning, land-use analysis, and the creation and maintenance of geographical databases [18]. For accurate map updating features were divided into two categories. First which has the correct position on the map (non-building features). The second one was high features (building) which were not at the correct position on the map because of their relief displacement. So, building areas were detected, to correct the relief displacement, by moving the rooftops borders.

Table2: change classes result between GeoEye-1image of 2014 and Sohag map2006.

Class	Area in Km2	% Of Total Study Area
N C	13.41	90.61%
V- U	0.263	1.78%
V- BS	0.093	0.63%
V- W	0.288	1.94%
V-R	0.041	0.28%
W-V	0.21	0.82%
BS-V	0.15	1.02%
BS-U	0.43	2.92%
Total	14.8	100%

## 5. Approximated method for relief displacement correction

Rectification of satellite data is one of the most important preprocessing steps for mapping applications and identifying a broader range of land or urban features [19]. For correcting the relief displacement, four stages were followed. First, rooftops of the building and shadow were extracted from the classified image. Second, the classified image was transformed from raster to vector format using ArcGIS 10.5 software. After that to move the building rooftops, the heights of buildings are estimated using the shadow length by ratio method [20]. Finally, a python code is written to calculate the new building rooftops coordinates.

### 5.1. Rooftops and Shadow detection

Building change detection has always been a popular direction in the field of remote sensing [21]. Automatic extraction of buildings from very-high-resolution (VHR) remote sensing imagery is a long-standing issue among the remote sensing research community [22]. Rooftops and the shadow of the buildings were extracted from the classified

image and arranged to buildings (rooftops), shadow and background as shown in figure 6.

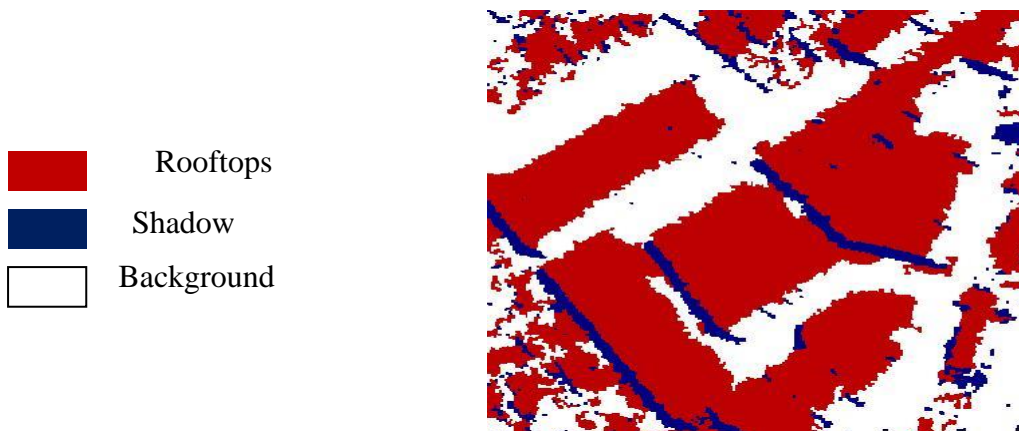


Figure 6: rearrangement of classification of the study area

## 5.2. vectorization

Once the change map was produced, the obtained results were transformed to vector format. Figures 7 and 8 show an example of the conversion of non-building and building features from raster to vector format. Many editing procedures were carried out on a vector layer to remove unnecessary edges in the lines by using smart raster to vector conversion tools in ERDAS 2013 program. These operations such as "Generalizing" can remove steps from the line and "Reshaping" can modify the shape of a single element after editing its nodes.

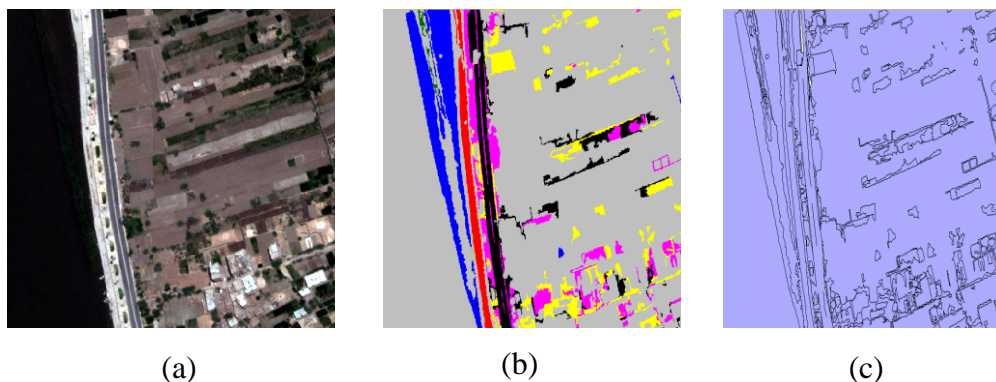


Figure 7: Raster to vector conversion of non-building features a) Original image b) Raster classified image and c) Vector format.

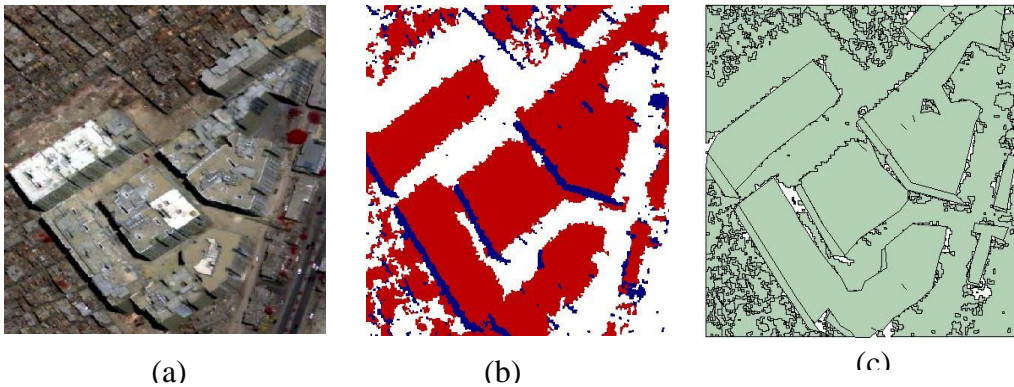


Figure 8: Raster to vector conversion of building features a) Original image b) Raster classified image and c) Vector format.

### 5.3. Building Height Estimation

Buildings are one of the most important types of artificial targets in the urban environment [23]. The height of the building can be calculated using the ratio method which was used in this research. The height of an unknown building is measured by taking the ratio of the height of reference building multiplied by the shadow length of the unknown building and the shadow length of the reference building as shown in equation 3.

$$H_{un} = (h_r * SL_{un}) / sl_r \dots\dots\dots (3)$$

where  $H_{un}$  and  $h_r$  are the height of the unknown building and the height of the reference building, respectively.  $SL_{un}$  and  $sl_r$  are shadow length of unknown and reference buildings (measured from the satellite Data) [18].

For calculating buildings' height, the length of a reference building had been measured using total station (SOKKIA CX 103). To estimate shadow length, shadow coordinates were extracted from the vector layer and exported to the excel program. Each building's shadow consists of four points. Shadow length was considered the smallest distance one of the four lines as shown in figure 9.



Figure 9. The height and shadow length of an unknown building

#### 5.4. Relief displacement calculation

For calculating the building's relief displacement as shown in figure 10, a python code was written [5]. The relief displacement can be calculated as follows:

$$L = H / \tan EL \quad (4)$$

where,  $L$ ,  $H$ , and  $EL$  are relief displacement, buildings height, and satellite elevation angle, respectively. Given an azimuth,  $AZ$ , the two components of the relief displacement  $\Delta E$  and  $\Delta N$ , can be determined by

$$\Delta E = L \sin AZ \quad (5)$$

$$\Delta N = L \cos AZ \quad (6)$$

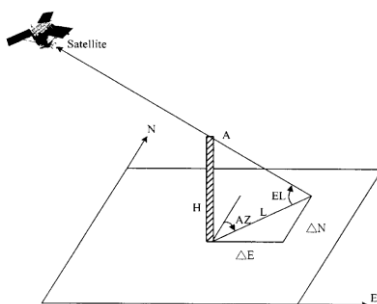


Figure 10: Relief displacement calculation (Chen, 2003).

After detecting rooftops as shown in figure 11, it moved according to shadow direction. In figure 11 points A1, A2, A3, and A4 were rooftop

corners at the wrong position. Points B1, B2, B3, and B4 were shadow corners and C1, C2, C3, and C4 were rooftop corners at the correct position as shown in figure 11. Shadow length was the distance between B1 and B2. Shadow length was calculated through the excel program. Direction from B4 to B3 was the direction to move rooftops to its correct position. Using buildings height and shadow length a python code was written to move the rooftops from wrong positions A1, A2, A3, and A4 to the correct positions C1, C2, C3, and C4.

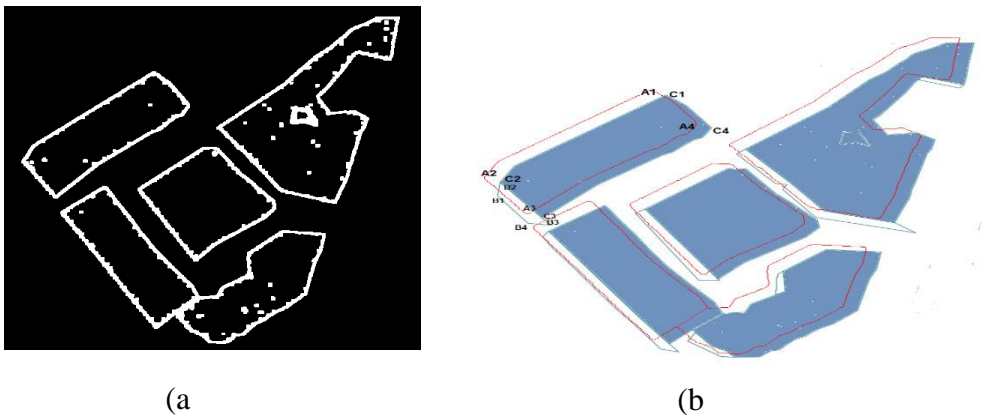


Figure 11: Python code resulted image a) Image preparation using python code.  
b) Moving rooftops to correct position according to buildings height

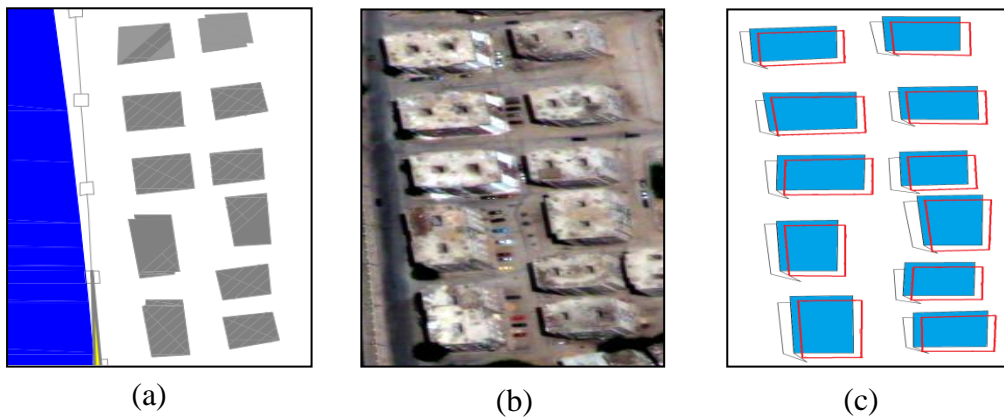


Figure 12: Moving rooftops for accuracy assessment of the approximated method  
(a) reference map (b) Original image (c) resulted image.

### 5.5. Accuracy assessment of the approximated method

The accuracy assessment evaluation was carried out using old buildings

which have already existed in the image and the map as shown in figure 12. Twenty buildings with 80 point which located at the no-change area were used. The chosen building's rooftops were corrected using the approximated method. The new position of rooftops and the reference building bases was measured to calculate the accuracy of the approximated method. The results showed that the RMSE was 0.95 meter.

## 6. Map Updating.

The most significant components of mapping from space images are geometric accuracy and information content. Data from the innovative parts of the change map vector features layer is inserted in the old data layer of the reference map to incorporate the new information as shown in figure 13. Using a python code, the rooftops of buildings were moved to the correct position (figure 14) according to building height and shadow length. Finally, the reference map was updated as shown in figure 15.

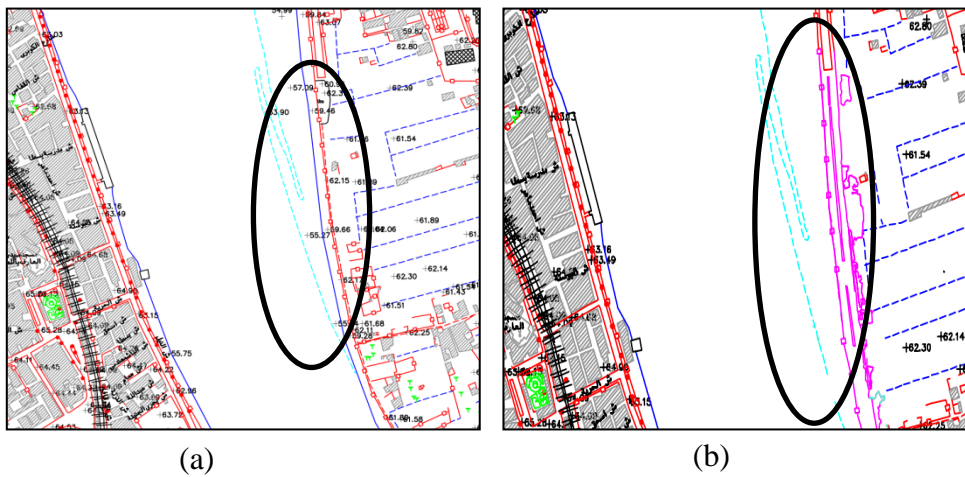


Figure 13: The updated reference Non-building map (a) reference map and (b) updated map.

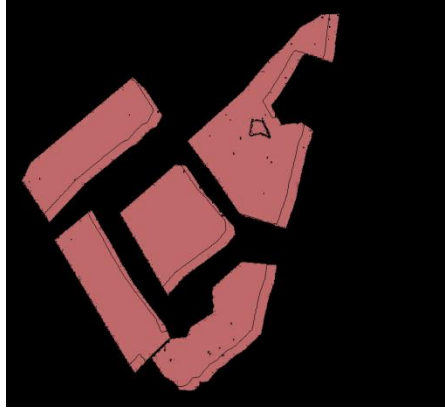


Figure 14: moving building's rooftops.



Figure 15: building map updating a) reference map b) updated map.

## 7. Discussion

Data preprocessing presented the satellite images in a more suitable form. The High-Pass Filter pan-sharpened method integrated PAN and MS images together and produced high spatial and spectral quality image. The geometric correction with third-order polynomial transformation has high accuracy with RMS errors in the checkpoints of 0.541 m. Studying information content for mapping on a 1:5000, or larger scale is problematic with a 1 m GSD. GeoEye-1 images, with 0.46 m GSD, can solve this problem. Object-based classification of GeoEye-1 image has high overall accuracy (90.67%) and Overall Kappa (0.88).

Post classification comparison was carried out between GeoEye-1 image and Sohag map. PCC method deals with classified images, so it

is a suitable method for change detection between images and maps. The PCC method producing a change matrix. It describes not only the amount of change but the type of changes that have occurred as well. The success of post-classification comparison depending on the accuracy of the classifications of the individual images. The change detection results show that transformation from bare soil to urban and vegetation to urban represented 2.41% of the total changes. This percentage indicated that urbanization occurred at a rapid rate in the last decade. The expansion of cities and villages in Egypt must be monitored almost annually to control the illegal construction of buildings.

Due to relief displacement, buildings appear in not accurate position in satellite images. Relief displacement calculation was a major step for the position correction of the building's rooftops mapping. A new approximated method for building relief displacement correction was developed. A python code was written to calculate relief displacement using buildings' height and shadow length. The results show that the average accuracy of the proposed method can reach 0.95 m. Maps should have a geometric accuracy of approximately 0.3 mm in the map scale according to the National Map Accuracy Standards (NMAS). For this scale map, the geometric accuracy of 1.5m ( $5000 \times 0.3\text{mm} = 1.5\text{m}$ ) is required. That means with 0.95m accuracy at a scale of 1: 5000 is a promising result. For more accuracy, we recommend the use of DSM for the orthorectification of the satellite image.

## **8. Conclusions**

Map updating is a very important issue in Egypt for better resource management. In this work, an approach for change detection between very high-resolution satellite images and maps is introduced. Also, an approximated method for relief displacement correction of building rooftops is developed. In correspondence with the results of the present work, it can be concluded that:

- The geometric accuracy and information content of GeoEye-1 image have the ability for updating Egyptian maps at a scale of 1:5000 according to the ESA.

- The PCC method can detect changes between images and maps with high overall accuracy and Kappa coefficient (89.60 % and 0.88 respectively). The percentage of change between 2006 map and 2014 VHR satellite image was found 9.39%. The highest percentage of change was found in class bare soil to urban (2.92 %).
- The developed approximated method for relief displacement correction gives high results with RMSE of 0.95m. The accuracy obtained meets the technical specifications of ESA for 1:5000 scale maps.

## References

- [1]. Hegazy, I.R. and Kaloop, M.R., 2015. Monitoring urban growth and land use change detection with GIS and remote sensing techniques in Daqahlia governorate Egypt. *International Journal of Sustainable Built Environment*, 4(1), pp.117-124.
- [2]. Jin, S., Yang, L., Danielson, P., Homer, C., Fry, J. and Xian, G., 2013. A comprehensive change detection method for updating the National Land Cover Database to circa 2011. *Remote Sensing of Environment*, 132, pp.159-175.
- [3]. Hu, Q., Zhen, L., Mao, Y., Zhou, X. and Zhou, G., 2021. Automated building extraction using satellite remote sensing imagery. *Automation in Construction*, 123, p.103509.
- [4]. Chen, H., Zhang, K., Xiao, W., Sheng, Y., Cheng, L., Zhou, W., Wang, P., Su, D., Ye, L. and Zhang, S., 2021. Building change detection in very high-resolution remote sensing image based on pseudo-orthorectification. *International Journal of Remote Sensing*, 42(7), pp.2686-2705.
- [5]. Chen, L.C., Lo, C.Y. and Rau, J.Y., 2003. Generation of digital orthophotos from IKONOS satellite images. *Journal of surveying engineering*, 129(2), pp.73-78.
- [6]. Comber, A., Umezaki, M., Zhou, R., Ding, Y., Li, Y., Fu, H., Jiang, H. and Tewkesbury, A., 2012. Using shadows in high-resolution imagery to determine building height. *Remote sensing letters*, 3(7), pp.551-556.
- [7]. Benarchid, O., Raissouni, N., El Adib, S., Abbous, A., Azyat, A., Achhab, N.B., Lahraoua, M. and Chahboun, A., 2013. Building extraction using object-based classification and shadow information in very high-resolution multispectral images, a case study: Tetuan, Morocco. *Canadian Journal on Image Processing and Computer Vision*, 4(1), pp.1-8.
- [8]. Zhang, L., B. Zhong, and A. Yang. 2019. Building change detection using object-oriented lbp feature map in very high spatial resolution imagery. In *Proceedings of 2019 10th International Workshop on the Analysis of Multitemporal Remote Sensing Images (Multitemp)*, 1–4. Shanghai, China.

- [9]. Technical specifications for the products and services of the Egyptian Survey Authority, Part 1: Topography and Geodesy, 2020.
- [10]. Dahiya, S., Garg, P.K. and Jat, M.K., 2013. A comparative study of various pixel-based image fusion techniques as applied to an urban environment. *International Journal of Image and Data Fusion*, 4(3), pp.197-213.
- [11]. Mostafa, Y., and A. Abedehafez. 2017a. Shadow Identification in High Resolution Satellite Images in the Presence of Water Regions. *Photogrammetric Engineering and Remote Sensing* 83 (2): 87–94
- [12]. Mostafa, Y., and A. Abedehafez. 2017b. Accurate Shadow Detection from High-Resolution Satellite Images. *IEEE Geoscience and Remote Sensing Letters* 14 (4): 494-498.
- [13]. Mostafa, Y. 2017. A Review on Various Shadow Detection and Compensation Techniques in Remote Sensing Images. *Canadian Journal of Remote Sensing* 43 (6): 545–562.
- [14]. Aguilar, M.A., Aguilar, F.J. and Agüera, F., 2008. Assessing geometric reliability of corrected images from very high-resolution satellites. *Photogrammetric Engineering and Remote Sensing*, 74(12), pp.1551-1560.
- [15]. Gungor, O. and Shan, J., 2004, July. Evaluation of satellite image fusion using wavelet transform. In proceedings of 20th Congress ISPRS “Geo-Imagery Bridging Continents (pp. 12-13), 12 - 23 July, Istanbul, Turkey.
- [16]. Alkan, M., Buyuksalih, G., Sefercik, U.G. and Jacobsen, K., 2013. Geometric accuracy and information content of WorldView-1 images. *Optical engineering*, 52(2), p.026201.
- [17]. Farrag, F.A., Mostafa, Y.G. and Mohamed, N.A., 2020. Detecting land cover changes using VHR satellite images: a comparative study. *journal of engineering science*, 48, pp.200-211.
- [18]. Li, J., Cao, J., Feyissa, M.E. and Yang, X., 2020. Automatic building detection from very high-resolution images using multiscale morphological attribute profiles. *Remote Sensing Letters*, 11(7), pp.640-649.
- [19]. Aguilar, M.A., del Mar Saldaña, M. and Aguilar, F.J., 2013. Assessing geometric accuracy of the orthorectification process from GeoEye-1 and WorldView-2 panchromatic images. *International Journal of Applied Earth Observation and Geoinformation*, 21, pp.427-435.
- [20]. Raju, P.L.N., Chaudhary, H. and Jha, A.K., 2014. Shadow analysis technique for extraction of building height using high resolution satellite single image and accuracy assessment. *International Archives of the Photogrammetry, Remote Sensing & Spatial Information Sciences*.
- [21]. Zhang, L., Zhong, B. and Yang, A., 2019, August. Building Change Detection using Object-Oriented LBP Feature Map in Very High Spatial Resolution Imagery. In 2019 10th International Workshop on the Analysis of Multitemporal Remote Sensing Images (MultiTemp) (pp. 1-4). IEEE.
- [22]. Feng, W., Sui, H., Hua, L., Xu, C., Ma, G. and Huang, W., 2020. Building extraction from VHR remote sensing imagery by combining an improved

- deep convolutional encoder-decoder architecture and historical land use vector map. *International Journal of Remote Sensing*, 41(17), pp.6595-6617.
- [23]. Ma, W., Wan, Y., Li, J., Zhu, S. and Wang, M., 2019. An automatic morphological attribute building extraction approach for satellite high spatial resolution imagery. *Remote Sensing*, 11(3), p.337.

## اكتشاف التغيرات لتحديث الخرائط باستخدام صور الأقمار الصناعية عالية الدقة

### الملخص العربي:

يتغير سطح الارض بشكل مستمر نتيجة للظواهر الطبيعية وبعض الانشطة الإنسانية، كما يعد التحضر السريع خاصة في الدول النامية واحدة من الموضوعات الهامة للتغير العالمي التي تواجه البشرية في القرن الحادي والعشرين. تظهر الاهداف التي ترتفع عن سطح الارض خاصة المباني في مكان غير صحيح في صور الاقمار الصناعية مقارنة بمكانها على الخريطة نتيجة للإزاحة النسبية، لذلك كان من المهم تصحيح اماكن المباني حتى يتسنى لنا انتاج خرائط دقيقة، ولذلك تم اقتراح طريقة لعمل التصحيح اللازم لهذه الازاحة النسبية. لتحديث الخريطة تم اولا اكتشاف التغيرات الحادثة بين خريطة سوهاج المنتجة سنة ٢٠٠٦ من قبل الهيئة المصرية للمساحة ومرئية القمر الصناعي GeoEye-1 الملتقطة سنة ٢٠١٤ باستخدام طريقة post-classification comparison. بعد الحصول على خريطة التغيرات تم تقسيمها إلى جزئين: مباني وأجزاء غير مبنية كما تم تحويل خريطة التغيرات من النظام النقطي raster إلى النظام المتجهي vector. بعد تحديد المباني والظلال بطريقة اوتوماتيكية من خلال التصنيف، تم قياس ارتفاعات المباني باستخدام طريقة ratio method ثم تم كتابة كود بايثون python code لحساب الازاحة النسبية وتصحيح اماكن المباني. وفي النهاية تم تقييم محتوى الصورة لتحديث الخريطة